Journal of Science and Technology
ISSN: 2456-5660 Volume 10, Issue 02 (Feb-2025)
www.jst.org.in *DOI:https://doi.org/10.46243/jst.2025.v10.i02.pp187-198*

Comparison of three triterpenoids' pharmacokinetic characteristics using UHPLC-MSMS after oral administration of a cucurbitacin tablet and nanosuspension

Dr.M.Kishore Babu[1],Sri. L. Ramachandra Reddy[2],
B. Sasidhar[3],K.Srirama Krishna[4]

1.Professor, Department of pharmaceutics, QIS College of pharmacy, Ongole, A.P
2.Assistant Professor, Department of pharmacognosy, QIS College of pharmacy, Ongole, A.P
3.Assistant Professor, Department of pharm.Biotech, QIS College of pharmacy, Ongole, A.P
4. Assistant Professor, Department of pharmacognosy, QIS College of pharmacy, Ongole, A.P

To Cite this Article
Dr.M.Kishore Babu,Sri. L. Ramachandra Reddy,B. Sasidhar,K.Srirama Krishna, **"Comparison of three triterpenoids' pharmacokinetic characteristics using UHPLC-MSMS after oral administration of a cucurbitacin tablet and nanosuspension.**" *Journal of Science and Technology, Vol. 10, Issue 02- Feb 2025, pp187-198*

Article Info
Received: 29-12-2024 Revised: 06-02-2025 Accepted: 17-02-2025 Published: 28-02-2025

Cucurbitacin, a triterpenoid chemical derived from Pedicellus Melo, is the principal active ingredient of cucurbitacin tablets (CUT) prescribed for the treatment of primary liver cancer and chronic hepatitis. Oral bioavailability of pharmacopotent compounds may be enhanced using nanosuspensions. The pharmacokinetics of three cucurbitacin triterpenoids (CuB, CuD, and CuE) after oral administration of CUT and a new P. Melo nanosuspension (MP-NPs) in rats have never been studied before.
Methods: The amounts of these cucurbitacin triterpenoids in the plasma were measured using UHPLC-MS/MS, which stands for ultra-performance liquid chromatography-tandem mass spectrometry. Using the positive ion mode for multiple reaction monitoring analysis, a sensitive, easy-to-use, and selective UHPLC-MS/MS technique was created. Waters Acquity HSS T3 (1.8 μm, 2.1 × 100 mm) was the chromatographic column used; the column temperature was 35 °C, and the flow rate was

0.3 mL/min, 5 μL injection volume, and a gradient elution of water (A) and methanol (B) was used as the mobile phase. The accuracy varied from -6.41% to -4.01% and the intra- and inter-day precision for all analytes was less than 13%. The data show that when the two groups of rats were given the same amount of CUT and MP-NPs orally, CuD and CuE had a longer elimination half-life (T1/2) than CuB, suggesting that CuB was eliminated more slowly. The triterpenoids in the MP-NPs group exhibited a considerable improvement in both Cmax and area under the plasma concentration compared to the CUT group, and they were able to attain Cmax in only 2 hours.
Discussion: When compared to traditional CUT, the MP-NPs formulation greatly improved the oral bioavailability of cucurbitacin triterpenoids. These results highlight the promise of nanosuspension technology for enhancing the pharmacokinetic profile of treatments based on cucurbitacin. Additional research and therapeutic use of cucurbitacin nanosuspensions may benefit greatly from the findings of this study.
Corresponding Author :M.Kishore Babu
Mail: kishorebabu.m@gmail.com

Introduction

cucurbitacin UHPLC-MS/MS rat plasma nanosuspension pharmacokinetics year 2021. For example, according to Xue et al., PVP K30 enhances artemisinin's transdermal permeability by inhibiting its crystallization.
According to Huang et al. (2019), Chen and Zheng (2014), Chen J et al. (2008), and He et al. (1994), cucurbitacin

tablets (CUT) have been used for a long time as a typical over-the-counter medicine to treat liver problems and related ailments. One of the main ingredients of cucurbitacin is a triterpenoid molecule, which is derived from plants in the Cucurbitaceae family. Through regulating signaling pathways including NF-κB, MAPK, and JAK/STAT, these drugs have potent anticancer effects. Among these actions, Park et al. (2015) noted that they limit the growth of tumor cells and induce apoptosis. In particular, CuB modulates several pathways, including JAK/STAT3, Nrf2/ARE, NF- κB, AMPK, MAPK, PI3K/Akt, CIP2A/PP2A, Wnt, FAK, Notch, and Hippo-YAP, to offer robust anti-inflammatory, antioxidant, antiviral, hypoglycemic, hepatoprotective, neuroprotective, and anticancer properties (Dai et al., 2023; Garg et al., 2018; Yesilada et al., 1988; Li et al., 2023; Lin et al., 2019; Yang et al., 2020; Kim et al., 2018; Lu et al., 2012; Chen R et al., 2008). Üremiş et al. (2022) and Ku et al. (2018) found that CuD stopped HepG2 cells from proliferating and caused them to die via regulating the JAK/STAT3, PI3K/Akt/mTOR, and MAPK pathways. CuE exerts anti-inflammatory, neuroprotective, anticancer, anti-apoptotic, anti-aging, and immunomodulatory effects by regulating pathways such as PI3K/Akt, NF-κB, FAK/AKT/GSK3β, TFAP4/Wnt/β-catenin, SIRT1/Nrf2/HO-1, miR-371b-5p/TFAP4, NF-κB/NLRP3, JAK/STAT, Jak/Stat3, ERK/MAPK, and PI3K/Akt/mTOR (Wang L et al., 2023; Zheng et al., 2022; Yang et al., 2022; Brouwer et al., 2020; Attard and Martinoli, 2015). Üremiş et al. (2023) found that it also promotes p62-dependent apoptosis, which in turn suppresses the growth of A549 human non-small-cell lung cancer cells. The low oral bioavailability of cucurbitacins, mostly due to their low water solubility and strong first-pass effects, limits the therapeutic applicability of these drugs (Hsu et al., 2023; Yu et al., 2014).

In traditional Chinese medicine, the dried peduncle of Pedicellus Melo fruits is used to cure inflammatory illnesses, phlegm retention, and jaundice. This crop is economically valuable because of the cucurbitacin it produces (Chen et al., 2024). Current research in pharmacology indicates that the principal active components of P. Melo, which are responsible for its medicinal properties, are abundant in the extract. These components include CuB, CuD, and CuE. Nevertheless, much like conventional cucurbitacin solutions, natural extracts have limited bioavailability and short systemic exposure due to their poor solubility in water and fast intestinal clearance.

Nano-drug delivery systems provide new ways to improve the bioavailability, stability, and solubility of pharmaceuticals that aren't extremely water-soluble. For instance, according to Lu et al. (2024), the bioavailability of Panax notoginseng saponin nanoparticles or nanoemulsions when taken orally is much enhanced. The solubility, dissolution, and bioavailability of breviscapine are all significantly improved in mice when given as a nanosuspension (Zhang et al., 2022). The polymer polyvinylpyrrolidone K30 (PVP K30) has been used for many components of traditional Chinese medicine, and it is often employed in nano-drug delivery systems (Waleka et al.,

Curcumin's stability and bioavailability are enhanced, while paclitaxel's solubility is improved by reducing its crystallinity (Shikov et al., 2009; Chen et al., 2021).

Thus, nanotechnology shows promise in resolving the issue of conventional herbal extracts' poor absorption efficiency. Because of their low solubility in water, the therapeutic use of CuB, CuD, and CuE is severely restricted. The majority of these compounds are still taken orally, but getting enough of the active chemicals to work is still a challenge. Consequently, there is a need to enhance their efficacy and user-friendliness by creating water-soluble formulations. An increase in bioavailability may be achieved by manufacturing nanodispersions, which enhance medication dispersion and solubility. Several pharmacological active components are inherently insoluble in water; however, by dispersing them in a solid, this may be greatly improved (Jacob et al., 2020; Wei et al., 2022; Fathi-Karkan et al., 2024; Wang L et al., 2017). The administration approach was optimized by preparing the P. Melo extract and then formulating MP-NPs using PVP K30. The next step was to examine the pharmacokinetic differences of CUT with MP-NPs. After that, pharmacokinetic experiments were performed on several formulations, and the extract was shown to include three triterpenoid chemicals with high content: CuB, CuD, and CuE. To our knowledge, this is the first research to compare the pharmacokinetics of CuB, CuD, and CuE in two different formulations; the results provide light on how the medication is absorbed and distributed throughout the body. Treatment plans may be fine-tuned with further knowledge about the drug's pharmacokinetics.

The purpose of this work is to provide a reliable and efficient method for the simultaneous analysis of CuB, CuD, and CuE, which are active components of both the CUT and MP-NPs groups, using bifendate as the internal standard (IS) (Figure 1). To further enhance the oral availability of insoluble medicines for clinical use, pharmacokinetic investigation was also conducted for the first time after a single oral dose of CUT and MP-NPs in rats.

Materials and methods

Materials

Shanghai Yuanye Biotechnology Co., Ltd. supplied the reference substances of cucurbitacin B (CuB; lot: Z02M7X10137; purity ≥98%), cucurbitacin D (CuD; lot: DSTDH008101; purity ≥98%), and cucurbitacin E (CuE;

lot: Z01M7S10309; purity ≥98%). The IS bifendate was acquired from Chengdu Must Bio-Technology in Chengdu, Sichuan Province, China (lot: 73536-69-3; purity ≥98%). The other chemical reagents, such as methanol and formic acid, were of HPLC grade and were supplied by Dikma Technologies of Beijing, China. John Melo

Instruments and UHPLC-MS/MS conditions

Working in tandem with an Agilent 1290 UHPLC system, the Agilent 6430 triple quadrupole mass spectrometer with an ESI source interface (Santa Clara, CA, United States: Agilent Technologies) was used. We also used a Waters ACQUITY HSS T3 Column (1.8 μm, 2.1 × 100 mm) from Waters, Manchester, UK, for the separations. Two different mobile phases, water (A) and methanol (B), were used to conduct gradient elution. For the following time intervals: 0.0–1.0 min, 80%–80% B; 1.0–1.5 min, 80%–90% B; 1.5–3.0 min, 90%–90% B; 3.0–3.2 min,

10% to 80% B; then 3.2% to 4% B for 3.2-4 minutes. At 35 °C, the analytical temperature was maintained, and 0.3 mL/min was the flow rate. The needle was cleansed after administering an injection with a volume of 5 μL.

The samples underwent positive ion-mode analysis. According to Wang et al. (2014), the desolvation temperature was set to 350 °C, the source temperature to 100 °C, and the capillary voltage to 4500 V. The nitrogen utilized for nebulizing and drying was high-purity nitrogen at a flow rate of 11 L/min. According to Wang Z et al. (2023), the experimental data was collected using the Agilent Mass Hunter workstation. Quantification was achieved using multiple reaction monitoring (MRM) mode under different fragmentor voltage (FV) and collision energy (CE) conditions listed in Table 1. The specific ion transitions for CuB, CuD, CuE, and IS were measured at m/z 581.2→521.9, m/z 539.3→480.2, m/z 578.9→520.9, and m/z 418.9→387.1, respectively. Presented in Figure 2 are the mass spectra of the three analytes and IS as they were produced.

Preparation of standards and QC samples

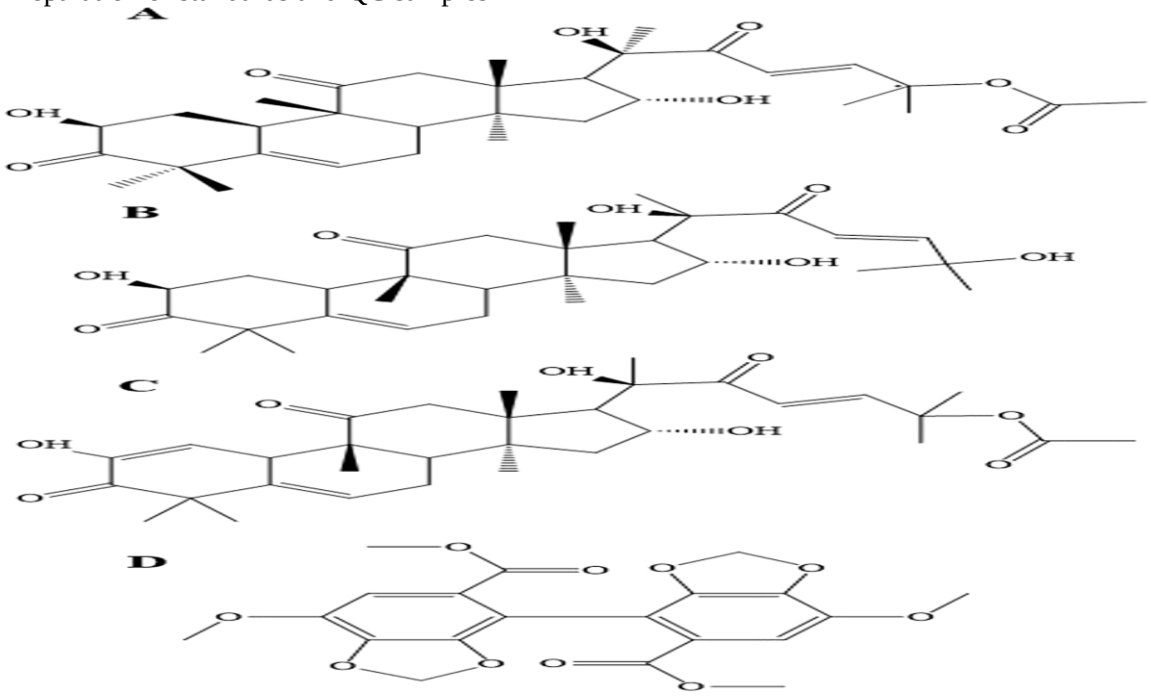

CuB (4.953 mg), CuD (4.603 mg), and CuE (4.544 mg) were accurately weighed and converted to 10 mL in methanol to prepare a single mother liquor of 0.4953, 0.4603, and 0.4544 mg/mL, respectively. The IS 5.504 mg was dissolved in methanol in a 20 mL volumetric flask, and a 0.275 mg/mL stock solution was obtained. The calibration solution was prepared by using the mother liquor gradient dilution method.
Following the necessary addition of blank plasma and standard solutions to the samples for the standard calibration curves, the final concentrations obtained were 2.109, 4.212, 10.50, 21.04, 42.10, 210.4, and 420.3 ng/mL for CuB; 10.08, 20.21, 50.52, 101.2, 202.7, 404.2,
and 808.2 ng/mL for CuD; 2.103, 4.221, 10.54, 21.13, 42.09, 210.3,
and 420.1 ng/mL for CuE. These concentrations were achieved by

TABLE 1 MRM parameters of the three analytes and IS.

Compounds	Transition	Fragmentor (V)	Collision energy (eV)	Quantifier ions	Polarity
IS	418.9→387.1	120	7	343.1	Positive
Cucurbitacin B	581.2→521.9	122	30	475.5	Positive
Cucurbitacin D	539.3→480.2	100	17	499.3	Positive
Cucurbitacin E	579.4→520.9	100	40	434.6	Positive

Pedicellus Melo nanosuspension preparation
A specific quantity of P. Melo was homogenized, and 8-fold volumes of methanol were added to the sample. The mixture was then subjected to three sequential ultrasonic extractions (for 40 min each) at room temperature. Following each extraction cycle, the
slurry was vigorously shaken, filtered through a 0.22 μm membrane
filter, and the filtrate was collected. The pooled filtrates were concentrated via rotary evaporation under reduced pressure to obtain the crude P. Melo extract. Simultaneously, a 20% (w/v) PVP K30 solution was prepared by dissolving the polymer in deionized water. The solution was magnetically stirred (600 rpm) at 60 °C in a water bath until a homogeneous, clear aqueous phase was achieved.

Animal experiments
A total of 12 male Sprague Dawley (SD) rats (weight: 220 ± 20 g) were provided by the Animal Experiment Center of Heilongjiang University of Traditional Chinese Medicine (Production license number: SYXK (Hei) 2021-010). The Laboratory Animal Ethics Committee of Heilongjiang University of Traditional Chinese Medicine approved the study (Approval No.: 2024053114).
Animals were randomly assigned to the following two experimental groups (n = 6 per group): CUT and MP-NPs. Treatments were administered once daily for seven consecutive days, with the plasma sampling performed at predetermined time points after administration. Dosage was calculated based on human- equivalent doses converted to rat pharmacokinetic parameters using interspecies scaling factors. The human-rat dose conversion procedure was used to determine the dose of CUT per rat to be
0.03 g. The recommended daily dosage for humans is 6 tablets. The dose of MP-NPs per rat was determined to be 0.06 g per rat using the human-rat dose conversion formula, whereas the dose of P. Melo for human usage was 3 g, with reference to the Pharmacopoeia of the People’s Republic of China 2025.

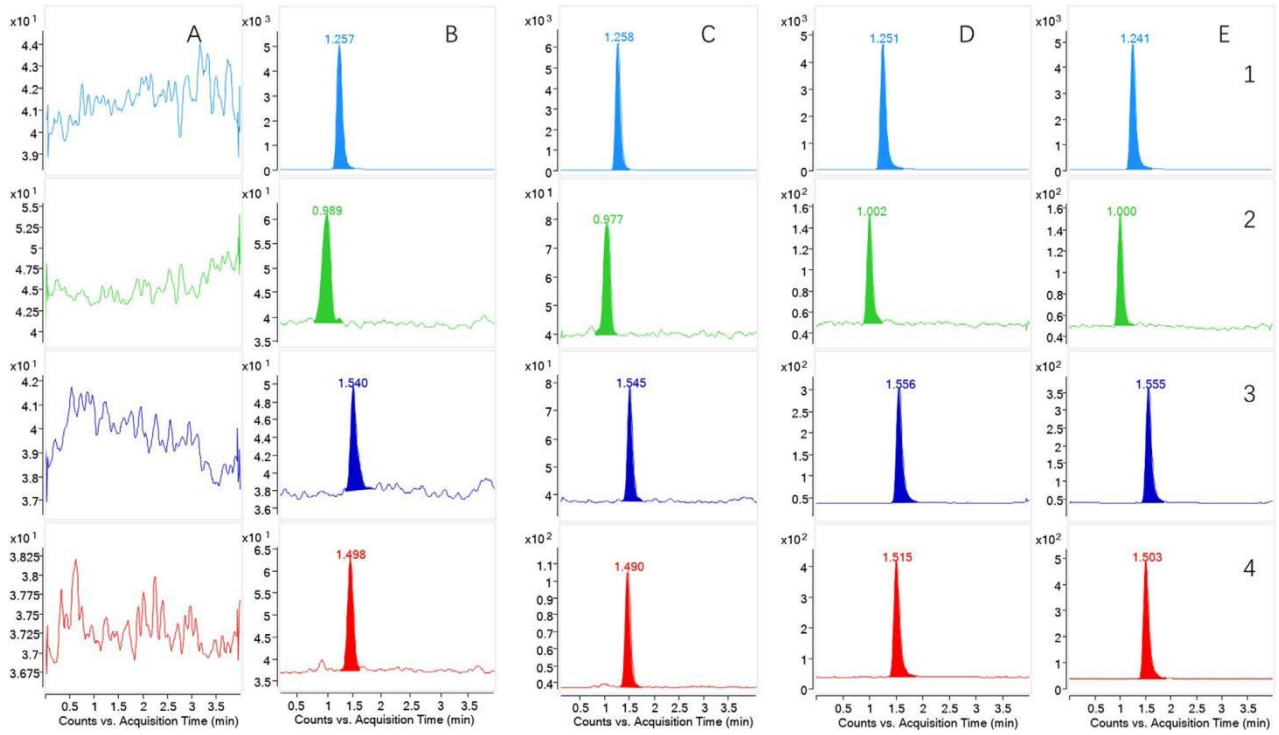

FIGURE 3
The chromatograms of the analytes in rat plasma. (1) IS; (2) Cucurbitacin D; (3) Cucurbitacin B; (4) Cucurbitacin E. (A) blank plasma; (B) plasma samples spiked with the analytes and IS at LLOQ; (C) blank plasma with the analytes and IS at MQC; (D) the plasma samples obtained at 2.5 h following the oral administration of CUT group (*n* = 6); (E) the plasma samples obtained at 2 h following the oral administration of MP-NPs (PVP-K30) group (*n* = 6).

TABLE 2 The calibration curves, linear ranges and LLOQs of three analytes.

Compounds	Regression equation	R2	Linear ranges (ng/mL)	LLOQ (ng/mL)
Cucurbitacin B	Y = 4.951*10−3X -3.680*10−2	0.9914	2.109–420.0	2.109
Cucurbitacin D	Y = 5.792*10−5X +1.240*10−2	0.9940	10.08–808.0	10.08
Cucurbitacin E	Y = 2.761*10−3X -2.023*10−2	0.9940	2.103–420.0	2.103

Results
Methods validation
Selectivity
Under the UHPLC-MS/MS conditions, the analyte was effectively separated. The IS, CuB, CuD, and CuE exhibited retention times of 1.258, 0.9890, 1.545, and 1.490 min, respectively. Figure 3 presents representative MRM chromatograms: (A) blank plasma; (B) plasma samples spiked with the analytes and IS at LLOQ; (C) blank plasma with the analytes and IS at MQC; (D) plasma samples obtained at 2.5 h after CUT was administered orally; and (E) plasma samples obtained at 2 h after MP-NPs were administered orally. These results confirmed that endogenous substances did not interfere with the analytes and IS during analysis.
Linearity and sensitivity
Table 2 presents the linear regression equations for quantification. All R2 exceeded 0.9914, demonstrating robust

linearity acrossthe validated concentration ranges. LLOQs for CuB, CuD, and CuE were 2.109, 10.08, and 2.103 ng/mL. These values fulfilled the sensitivity requirements for pharmacokinetic analysis.

Precision and accuracy

Precision and accuracy were evaluated by analyzing QC samples at four concentrations: LLOQ, LQC, MQC, and HQC. Intra- and inter-day precision were assessed over three consecutive days. For all three analytes (CuB, CuD, and CuE), the precision values remained below 13% for both intra- and inter-day measurements, meeting the acceptance criteria for validation using the bioanalytical method. Accuracy, expressed as RE%, ranged from −3.987% to 9.047% across all QC levels (Table 3). Negative RE values indicated slight underestimation, whereas positive values reflected overestimation relative to nominal concentrations. These results unveiled that the analytical procedure was reliable and accurate for quantifying cucurbitacins in biological matrices.

TABLE 3 The intra-day and inter-day precisions and accuracies of the three analytes (n = 6).

Compounds	Spiked concentration (ng/mL)	Measured concentratio (ng/mL)	Intra-day		Inter-day	
			Accuracy (RE %)	Precision (RSD %)	Accuracy (RE %)	Precision (RSD %)
CuB	2.109	2.213 ± 0.2721	−2.243	9.053	8.373	12.43
	5.272	5.202 ± 0.4821	1.722	8.042	2.026	9.193
	150.1	147.3 ± 6.861	−1.054	3.974	−1.882	4.662
	300.2	288.2 ± 16.12	−2.453	4.074	−3.987	5.592
CuD	10.10	9.942 ± 1.114	−6.131	12.97	−1.803	11.19
	25.25	24.90 ± 2.060	−5.074	7.376	−1.584	8.264
	300.1	295.8 ± 9.022	−0.802	3.364	−1.422	3.051
	600.2	590.9 ± 16.80	−1.833	2.332	−1.554	2.845
CuE	2.103	2.082 ± 0.2021	−1.542	6.590	5.895	9.648
	5.257	5.341 ± 0.4913	6.701	10.41	9.047	9.112
	150.4	147.7 ± 6.652	−1.373	1.914	−1.775	4.501
	300.8	289.1 ± 21.71	−5.322	9.075	−3.903	7.518

TABLE 4 Matrix effect and extraction recovery for the three analytes (n = 6).

Compounds	Spiked concentration (ng/mL)	Extraction recovery		Matrix effect	
		Mean (%)	RSD (%)	Mean (%)	RSD (%)
CuB	5.272	86.56	7.512	99.65	11.98
	150.1	89.79	6.023	106.3	4.553
	300.2	93.69	6.425	100.3	9.053
CuD	25.30	79.23	5.997	99.72	11.60
	300.1	82.78	6.542	97.80	9.674
	600.2	83.20	10.52	103.3	6.522
CuE	5.257	83.50	10.37	99.20	7.505
	150.4	87.93	10.19	101.4	5.142
	300.8	91.87	7.881	97.02	9.794

Extraction recovery and matrix effect

Table 4 presents the extraction recoveries of the three analytes across three QC levels, which ranged from 86.56% to 93.69%, 79.23%–83.20%, and 83.50%–91.87%, respectively. The matrix effects for the three analytes ranged from 97.02% to 106.3%. These results revealed negligible matrix effects on the analytes, indicating the appropriateness of the extraction solvent used.

Stability

Table 5 outlines the stability of LQC, MQC, and HQC in the rat plasma under different storage conditions. CuB, CuD, and CuE remained stable under the following conditions: storage at −20 °C, ambient temperature (25 °C) for 4 h, three freeze-thaw cycles (−20 °C/ room temperature) over 2 weeks, and 12 h storage at 4 °C post-sample preparation. The RSD for these conditions was ≤11.01%, confirming
minimal variability. Thus, the analytes were not significantly degraded throughout all stages of sample handling and analysis.

Pharmacokinetic studies

The established UHPLC-MS/MS method was applied to simultaneously measure the plasma concentrations of the three analytes in rats following dose administration. Pharmacokinetic parameters have attracted attention in exploring drug absorption and distribution. These parameters include T1/2, Cmax, Tmax, and AUC (Table 6). The average plasma concentration-time curve is presented in Figure 4. The pharmacokinetics of SD rats following oral administration of CUT and MP-NPs were investigated through UHPLC-MS/MS. The plasma concentrations of the three analytes

TABLE 5 The stability of the three analytes under different storage conditions (n = 6).

Compounds	Spiked concentration	Stability (RE%)			
	(ng/mL)	Post-preparative	Short-term	Long-term	Freeze-thaw
CuB	5.272	−6.702	−6.465	4.471	−3.215
	150.1	−10.45	−3.932	−11.01	−7.542
	300.2	−8.081	−6.496	−8.414	−6.654
CuD	25.30	−3.854	4.262	5.336	−3.242
	300.1	−8.805	−4.154	−5.533	−8.420
	600.2	7.032	−5.861	−2.272	−7.765
CuE	5.257	6.711	6.050	8.213	7.947
	150.4	−2.053	−4.192	5.814	1.424

	300.8	−8.572	−3.143	−3.035	−1.361

TABLE 6 Pharmacokinetic parameters of the three compounds in the CUT group and the MP-NPs group rat plasma after oral administration of cucurbitacin tablet and MP-NPs(PVP-K30) (n = 6, mean ± SD). (Note: * for $p < 0.05$, and ** for $p < 0.01$).

Compounds	Group	Cmax (ng/mL)	Tmax (h)	T1/2 (h)	AUC0→t (ng·h/mL)	AUC0→∞ (ng·h/mL)
CuB	CUT	142.1 ± 22.24	2.421 ± 0.3810	4.871 ± 1.121	617.9 ± 88.56	708.1 ± 77.29
	MP-NPs	228.6 ± 11.97**	1.922 ± 0.3831*	4.569 ± 1.033	875.5 ± 217.1*	975.7 ± 255.4*
CuD	CUT	338.8 ± 24.37	1.832 ± 0.6834	5.328 ± 0.9912	1,033 ± 167.2	1,157 ± 167.8
	MP-NPs	364.7 ± 69.88*	1.752 ± 0.6102	6.967 ± 2.923	1,259 ± 260.9*	1,481 ± 225.8*
CuE	CUT	166.2 ± 13.84	2.253 ± 0.5206	5.991 ± 1.230	602.9 ± 125.4	682.3 ± 126.3
	MP-NPs	236.3 ± 31.87**	1.674 ± 0.6121*	7.053 ± 2.701	751.6 ± 149.6*	972.6 ± 268.7*

were calculated. The Tmax values of these analytes gradually increased. The MP-NPs group reached Cmax more rapidly than the CUT group. AUC0→t and AUC0→∞ also demonstrated that MP-NPs were superior to CUT preparations, suggesting that MP-NPs had higher AUC in vivo, possibly due to the increased drug bioavailability and absorption by the nanoparticles, thereby enhancing drug accumulation in the body.

Discussion

Optimization of UHPLC-MS/MS conditions

Mass spectrometric conditions, including ionization and parameters, were first optimized. A higher response was observed in the ESI positive-ion mode than in the negative-ion mode. Mass spectral parameters of the compounds varied based on the instrument and operating conditions (Abdollahi et al., 2024; Bali et al., 2011; Aluri et al., 2023). The MRM mode was employed for testing the precursor and product ions of the three compounds and IS to ensure reliability. Optimal ion transition pairs for quantitation were identified: m/z 581.2→ 521.9 for CuB, m/z 539.3→ 480.2 for CuD, m/z 578.9→ 520.9 for CuE, and m/z 418.9→ 387.1 for IS in the MRM mode. The effects of different mobile phase combinations (acetonitrile–water and methanol–water) and buffers (ammonium formate, formic acid, ammonium acetate, and acetic acid) on chromatographic behavior were examined. The mobile phase selected was methanol–water, with a column temperature and flow rate of 35 °C and 0.3 mL/min, respectively. The injection volume was 5 μL, and the total run time was 4 min.

Selection of IS

An appropriate IS with good stability that remains unchanged during sample processing and analysis must be selected for biological sample analysis. An unstable IS may lead to errors in the quantitative analysis. This study explored the effects of m-nitrophenol and bifendate as potential IS. When bifendate was detected in the positive-ion mode, it had a retention time with a significant separation from the analyte, generating symmetrical and sharp peaks, which indicated its stability and sensitivity. Therefore, the bifendate was selected as the IS in the experiment.

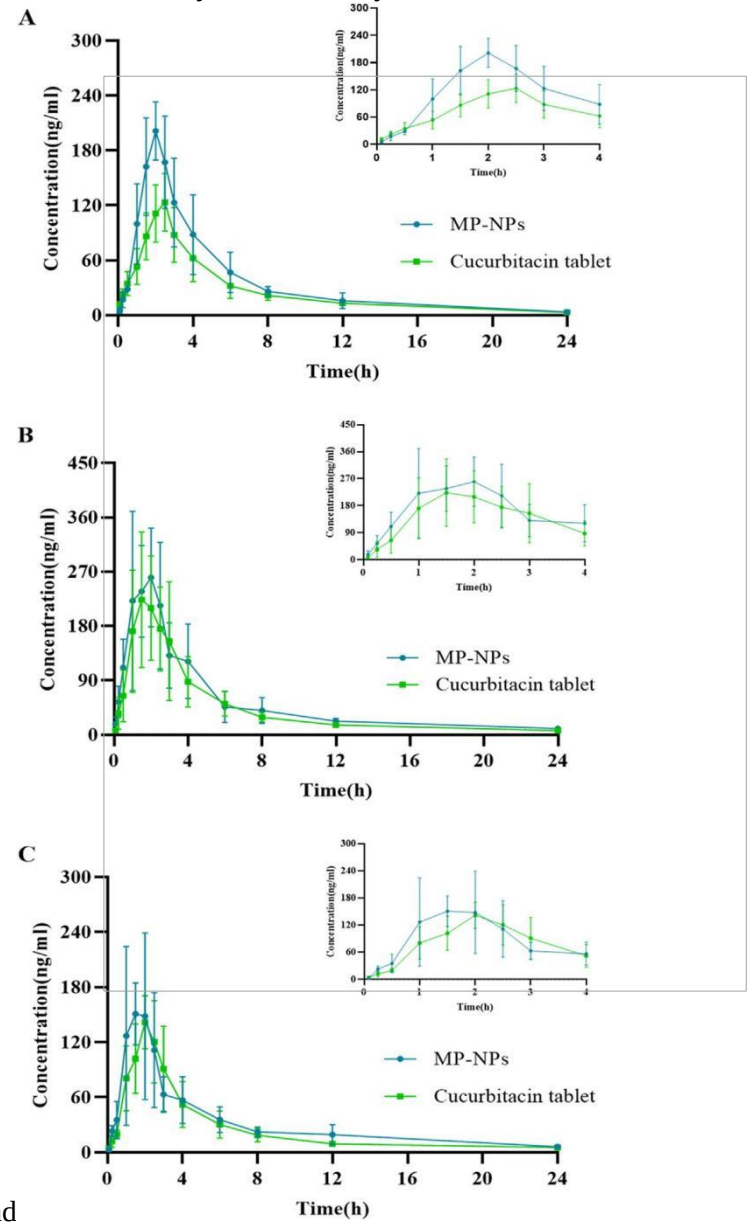

And

CuI all had cucurbitane-type triterpenoid parent nuclei, but exhibited varying substituents, affecting solubility and bioavailability. CuI is well-known for exerting powerful anti- cancer properties, particularly by regulating the JAK/STAT and PI3K/Akt pathways (Xu et al., 2022; Üremiş et al., 2022; Zhu et al., 2018). CuB, CuD, and CuE also exert equally strong anti-cancer, hepatoprotective, and anti-inflammatory effects compared with CuI. In P. Melo, the content of CuB, CuD, and CuE was significantly higher than that of CuI, and pharmacokinetic data on CuB, CuD,

and CuE (especially components in TCM nanosuspensions) in P. Melo remain scarce. Our MP-NP formulations specifically address the bioavailability limitations of these understudied cucurbitacins. Therefore, this study primarily investigated the pharmacokinetics of CuB, CuD, and CuE nanosuspensions. The pharmacokinetic studies revealed that MP-NPs were substantially advantageous over CUT in terms of the drug absorption rate, Cmax, AUC, and T1/2, possibly because of the nanosuspension characteristics of MP-NPs (such as larger surface area, higher solubility, and slower drug release). These characteristics can improve drug bioavailability and prolong its action time in the body. For example, the MP-NPs group reached Cmax more quickly after absorption than the CUT group ($P < 0.05$), potentially because of the nanosuspension characteristics of MP-NPs. MP-NPs may have better bioavailability or higher solubility, and so, the drug is more easily absorbed into the bloodstream. For CuD and CuE, the T1/2 of MP-NPs was generally longer than that of CUT. For instance, the T1/2 of CuD was 6.967 h (MP-NPs) versus 5.328 h (CUT), and for CuE, it was
7.053 h (MP-NPs) versus 5.991 h (CUT). This suggests that nanosuspension formulations have a longer retention time in the body, likely due to their physicochemical properties, which allow for
slow release. AUC values of the three compounds were significantly higher in the MP-NPs group ($P < 0.05$). $AUC_{0\rightarrow t}$ for CuB was
875.5 ng·h/mL (MP-NPs) versus 617.9 ng·h/mL (CUT). It was
1,259 ng·h/mL (MP-NPs) versus 1,033 ng·h/mL (CUT) for CuD and 751.6 ng·h/mL (MP-NPs) versus 602.9 ng·h/mL (CUT) for CuE (Abdollahi et al., 2024; Bali et al., 2011). This suggests that MP-NPs have a higher AUC, likely because their nanosuspension enhances the drug's bioavailability and absorption rate in the body, thereby increasing drug accumulation.
Because of the polymeric nature of PVP K30, a high-molecular- weight stabilizer used for MP-NPs preparation, MP-NPs significantly improved triterpenoid solubility, likely due to reduced drug particle size and the increased specific surface area (Abdollahi et al., 2024; Bali et al., 2011; Aluri et al., 2023; Wang Z et al., 2017; Sun et al., 2024; Zhang, 2018; Roos et al., 2017; Wang et al., 2020). PVP K30 stabilizes the nanocrystal system primarily through steric hindrance. Its long polymer chains adsorb onto the nanoparticle surfaces, forming a physical barrier preventing particle aggregation through steric repulsion. This spatial barrier effectively counters attractive forces (e.g., van der Waals forces) between nanocrystals, thereby preserving their reduced size and preventing agglomeration, which is crucial for maintaining the high specific surface area and the resultant increased solubility. It is also crucial for improving its dissolution rate and promoting absorption. This experiment offers a valuable reference for the exploration of various dosage forms. The toxicology and pharmacodynamics of this preparation will be explored to continue to improve nanosuspension-related research data.

Conclusion

In this work, we created and verified a sensitive, accurate, stable, and precise UHPLC-MS/MS technique that handles matrix effects, extraction recovery, and precision and accuracy admirably. After oral dosing, this approach was utilized to quantify CuB, CuD, and CuE concentration in rat plasma, CUT, and MP-NPs all at once. When compared to CUT, MP-NPs, a nanosuspension dispersion technology, greatly increased the three triterpenoids' oral bioavailability and, by extension, their plasma levels. The findings pave the way for future clinical trials to compare various dose forms in terms of release time, absorption rate, and metabolism.

References

In 2024, Abdollahi, Raissi, and Farzad published a document. To address the issue of low drug solubility, investigate nanosuspensions stabilized with polyvinyl alcohol using molecular dynamic modeling. Publication number: 14, 17386. DOI: 10.1038/s41598-024-68362-2. I
These authors collaborated in 2023: Aluri, Sigfridsson, Xue, Hariparsad, McGinnity, and Ramsden. Investigation of the pharmacokinetics of nano- or microcrystal formulations of insoluble substances after intraperitoneal administration in mice. International Journal of Pharmaceutical Sciences, 636, 122787, doi:10.1016/j.ijpharm.2023.122787.
In 2015, Attard and Martinoli published a paper. An experimental lead triterpenoid, cucurbitacin E has unique actions against degenerative disorders, modulates the immune system, and fights cancer. A brief analysis. Current Topics in Medical Chemistry 15, 1708–1713. doi:10. 2174/1568026615666150427121331.

Volcano Bali, Mausoleum Ali, and Jahangir Ali (2011). Evaluation of a nanocarrier for improved bioavailability of a cardiovascular agent: in vitro, pharmacodynamic, pharmacokinetic, and stability studies. International Journal of Pharmaceutical Sciences 403, 46–56. doi:10.1016/j.ijpharm.2010.10.018.
In 2020, the authors Brouwer, Out-Luiting, Vermeer, and Tensen published a paper. Sézary cells are programmed to die when exposed to cucurbitacin E and I, which target the JAK/STAT pathway. Science Direct, Volume 24, Issue 100832, doi:10.1016/j.bbrep.2020.100832
In 2014, Chen and Zheng published a paper. Results from clinical trials of fuzheng Huayu cucurbitacin tablets for the treatment of non-alcoholic fatty liver disease in children with fibrosis of the liver. Clinical Ratio of Drug Use7, 49–50. doi:10.15887/j.cnki.13–1389/r.2014.16.009.
The authors of this work are Chen Y., Wang J., Rao Z., Hu J., Wang Q., Sun Y., and others (2022). Research on the stability and bioavailability of curcumin-loaded (-)-epigallocatechin-3-gallate/poly (N-vinylpyrrolidone) nanoparticles produced by hydrogen bonding-driven self-assembly in oral administration. The published version of this article is 378 pages long and has the DOI: 10.1016/j.foodchem.2022.132091.
In 2024, Chen, Pan, Xu, and Gao published a paper. Investigations into the pharmacological effects and chemical components of Cucumis plants have advanced.
Journal of Liaoning University of Traditional Chinese Medicine 26, 2041–2025, doi:10.13194/j.issn.1673–842x.2024.01.038.
In 2008, a group of researchers known as Chen et al. Hemsleya endecaphylla tuber triterpenoids octanorcucurbitane and cucurbitane suppress HIV-1. Journal of Natural Products 71, 153–155. doi:10.1021/np0704396.
R. H. Chen, J. Z. Gong, and L. W. Xu (2008). Curcumin pill treatment of fifty instances of chronic hepatitis B: a clinical observational study. Number 23, pages 688-689, Primary Medical Forum.
Authors: Dai, S., Wang, C., Zhao, X., Ma, C., Fu, K., Liu, Y., and others (2023). Cucurbitacin B: a clinical, toxicological, and pharmacokinetic study. Journal of Pharmaceutical Research, 187, 106587 (doi:10.1016/j.phrs.2022.106587).

An article published in 2024 by Fathi-Karkan, Amiri Ramsheh, Arkaban, Narooie-Noori, Sargazi, Mirinejad, and others. Overcoming obstacles and improving medicine delivery for eye illnesses using nanosuspensions in ophthalmology. International Journal of Pharmaceutical Sciences, 658, 124226, doi:10.1016/j. ijpharm.2024.124226.
Published in 2018 by Garg, S. C., Kaul, R., and Wadhwa, R. The chemical, biological, and mechanistic aspects of cucurbitacin B's cancer intervention (Review). International Journal of Oncology, 52, 19–37. doi:10.3892/ijo. 2017.4203.
In 1994, He, J. J., Zhu, D., and Tian, L. Results from 89 patients treated with cucurbitacin pills for chronic hepatitis B. Journal of the Zhejiang College of Traditional Chinese Medicine 4, 18–19. doi:10. 16466/j.issn1005-5509.1994.04.014.
A group of researchers including Hsu, Lin, Tu, Nguyen, and Wang (2023) have published a study.
Human non-small-cell lung cancer A549 cells are subjected to cucurbitacin E's anti-proliferative effects via the promotion of p62-dependent apoptosis. Volume 45, Issues in Molecular Biology, pages 8138–8151, doi:10.3390/cimb45100514.
Xiao, M. S., Huang, Y., and Wu, H. L. (2019). Curcumin tablet's protective properties against rat non-alcoholic fatty liver disease. This article was published in the Zhejiang Medical Journal and has the DOI:10.12056/j. issn.1006-2785.2019.41.8.2018-2387. Its pages number 417–742.
A. B. Nair, J. Shah, and S. Jacob (2020). Nanosuspensions' potential in medication delivery systems is only beginning to emerge. Research in Biomaterials 24, 3 doi:10.1186/s40824-020-0184-8
Lee, I. S., Kim, Y., Jang, H. J., Park, J. Y., and Kim, K. H. (2018). via the modulation of AMP-Activated protein kinase alpha and glucagon-like Peptide-1 via bitter taste receptor signaling, cucurbitacin B generates a hypoglycemic effect in diabetic mice. Publication date: "Front. Pharmacol. 9, 1071." DOI: 10.3389/fphar.2018.010871.
J. M. Ku, S. H. Hong, H. I. Kim, Y. S. Lim, S. J. Lee, M. Kim, and others (2018).
By blocking Stat3 and Akt signaling, cucurbitacin D demonstrates its anti-cancer effects in human breast cancer cells. The article is published in the European Journal of Inflammation and has the DOI: 10.1177/ 1721727X17751809-10.
As a group, Li et al. (2023) include Yao Y., Li H., Gao C., Sun C., and Li Y. The anticancer medication cucurbitacin: a potential candidate. The publication comes from Biomed. Pharmacother and has the DOI:

10.1016/j.biopha.2023.115707.
In 2019, Lin et al. were joined by Kotakeyama and Li as well as Pan and Matsuura and Ohya. By controlling autophagy and oxidative stress, cucurbitacin B slows the aging process in yeast. The article is published in the journal Oxid. Med. Cell. Longev. and has the DOI of 5017091.
Citation: Lu, P., Yu, B., & Xu, J. (2012). Patients with lung cancer benefit from enhanced antitumor immunity and cucurbitacin B's regulation of immature myeloid cell development. Research in oncology and allied radiopharmaceuticals 27, 495–503 doi:10.1089/cbr.2012.1219.
(Wang, X., Lu, W. M., & Wang, X. T., 2024). The bioavailability of saponins from Panax notoginseng has been enhanced by recent advances in innovative formulation methods. Tianjin Journal of Traditional Chinese Medicine, 41, 672-680, doi:10.11656/j.issn.1672-1519.2024.05.21.
In 2015, a group of researchers including Park, G., Kim, Y. S., Lee, S. J., and Leem, K. worked together.
By activating Nrf2/ARE and inhibiting STAT/NF-κB, cucurbitacins reduce microglial activation and shield neurons from neuroinflammatory damage. The Neuroscience Letters, 609, 129–136, doi:10.1016/j.neulet.2015.10.022.
The authors of the article are Roos et al. (2017) and Dahlgren et al. Exploring the in vivo processes of aprepitant nanoformulation-induced gastrointestinal medication absorption. Chemical and Pharmaceutical Research 14, 4233–4242. doi:10.1021/acs.molpharmaceut. 7b00294
Contributors: A. N. Shikov, O. N. Pozharitskaya, I. Miroshnyk, S. Mirza, I. N. Urakova, S. Hirsjärvi, and others (2009). Effects of solid-state characteristics on the solubility of taxifolin nanodispersions. International Journal of Pharmaceutical Sciences 377, 148–152. doi:10.1016/j.ijpharm.2009.04.044.
Zhang, Y., Lu, J., Sun, J., An, W., Wang, S., and Zhao, Z. (2024). By blocking NLRP3 inflammasome-mediated pyroptosis, oxyymatrine reduces ulcerative colitis. Report number: 29, and the DOI is 10.3390/molecules29122897.
In 2022, Üremiş et al. were joined by Tosun, Çiğremiş, Baysar, Üremiş, M. M., and Durhan. By influencing the MAPK, PI3K/Akt/mTOR, and JAK/STAT3 signaling pathways, cucurbitacin D promotes apoptosis and suppresses HepG2 cell growth. Current Cancer Drug Targets 22, 931-944. doi:10.2174/1568009622666220623141158.
Üremiş, N., Türköz, Y., and Üremiş, M. M. (2023). By simultaneously triggering cell death in hepatocellular carcinoma cells, cucurbitacin E and sorafenib have a synergistic impact.